CLINICAL AND VACCINE IMMUNOLOGY, Nov. 2006, p. 1237–1245 Vol. 13, No. 11
1556-6811/06/$08.00+0 doi:10.1128/CVI.00184-06

Human Immunodeficiency Virus Persistence and Production in T-Cell Development▽

Kevin B. Gurney[1]† and Christel H. Uittenbogaart[1,2]*

Department of Microbiology, Immunology, and Molecular Genetics[1] and Department of Pediatrics,[2] UCLA AIDS Institute, Jonsson Comprehensive Cancer Center, David E. Geffen School of Medicine at UCLA, Los Angeles, California

Received 22 May 2006/Returned for modification 28 June 2006/Accepted 12 September 2006

Human immunodeficiency virus type 1 (HIV-1) replication depends on CD4 and coreceptor expression as well as host factors associated with the activation state of the cell. To determine the impact of the activation stage of thymocytes on the HIV-1 life cycle, we investigated R5 and X4 HIV-1 entry, reverse transcription, and expression in discrete thymocyte subsets at different stages of T-cell development. Early after infection, preferential entry and replication of R5 HIV-1 were predominantly detected in mature $CD3^{+/hi}$ $CD27^{+}$ thymocytes. Thus, R5 HIV-1 targets the stage of development where thymocytes acquire functional responsiveness, which has important implications for HIV pathogenesis. In contrast, X4 HIV-1 expression and replication were primarily found in immature $CD3^{-/+/low}$ $CD27^{-}$ $CD69^{-}$ thymocytes. HIV-1 proviral burden and virus expression in thymocyte subsets correlated with the expression of the highest levels of the respective coreceptor. R5 and X4 HIV-1 entered and completed reverse transcription in all subsets tested, indicating that the activation state of thymocytes and coreceptor expression are sufficient to support full reverse transcription throughout development. Although R5 HIV-1 is expressed mainly in mature $CD3^{+/hi}$ $CD27^{+}$ thymocytes, 5.3% of HIV-1-infected immature thymocytes express R5 HIV-1, indicating that potentially latent viral DNA can be established early in T-cell development.

Human immunodeficiency virus type 1 (HIV-1) entry involves sequential interactions of the viral envelope proteins with CD4 and chemokine receptors, primarily CCR5 or CXCR4 (11, 12, 15). With over 90% of developing cells in the thymus expressing CD4, the determining factor for HIV-1 infection in the thymus is the expression of the appropriate chemokine receptor or coreceptor. We and others have described the predominance of CXCR4 expression over CCR5 expression in the thymus, which facilitates the greater entry levels, faster replication kinetics, and enhanced cytopathicity of CXCR4 (X4)-tropic over CCR5 (R5)-tropic viruses in the human thymus (10, 18, 27, 40). Although the levels of CCR5 in the thymus are low, simian immunodeficiency virus studies have shown that the thymus is an important target for R5 virus (17, 30, 36, 49). Sopper et al. found an increase in mature thymocytes in the asymptomatic phase of simian immunodeficiency virus infection, with a severe depletion of mature CD4 and CD8 thymocytes in the symptomatic phase of infection, indicating impairment of T-cell regeneration (36). In addition to entry, the activation state of the host cell is a determining factor for HIV-1 replication.

Cellular activation can either enhance or restrict HIV-1 replication at multiple stages of the viral life cycle (23, 45). Completion of reverse transcription in vitro is dependent on the activated state of the host cell at or beyond the G_1b phase of the cell cycle (21, 50, 51). Cell-type-specific replication barriers also exist; for example, X4 HIV-1 is reportedly blocked at the level of nuclear import in Th2 T-cell clones (47). Furthermore, a lack of X4 replication and pathogenicity has been observed in the SCID-hu peripheral blood lymphocyte model, in which virus is injected into SCID mice 2 weeks after peripheral blood lymphocyte transfer, when the cells exhibit a memory phenotype (14). Monocytes, macrophages, and dendritic cells also exhibit activation/maturation-related blocks in HIV-1 replication (4, 33).

T-cell development in the thymus is an active process of positive and negative selection (37, 48). Given the diverse types of signals received by thymocytes during development, specific developmental stages may be more or less permissive for virus replication than others. Thus, HIV-1 pathogenesis in the thymus may be better understood by investigating the replicative capacity of HIV-1 in thymocytes at distinct developmental stages and by examining HIV-1 replication at the activation-dependent steps of the viral life cycle within the thymus. Although HIV-1 expression in major thymocyte subsets has been reported, an in-depth analysis of entry and reverse transcription in distinct thymocyte subsets, in particular of thymocytes to be exported to the periphery, is still lacking.

We report here that thymocytes are sufficiently activated to support HIV-1 replication at the five distinct differentiation and activation stages that we examined. Both R5 and X4 HIV-1 entered and completed reverse transcription in each developmental subset studied. However, R5 HIV-1 replication in vivo predominated in the functionally mature $CD27^{+}$ thymocyte subset while X4-HIV-1 replicated primarily in the $CXCR4^{+/hi}$ $CD69^{-}$ (pre-positive-selection) stage of development and was highly productive in the $CD3^{-/dim}$ $CD71^{+}$ cycling cells.

MATERIALS AND METHODS

Reagents and mAb. The serum-free medium consisted of Iscove's modified Dulbecco's medium (IMDM; Omega Scientific, Tarzana, CA) supplemented

* Corresponding author. Mailing address: Department of Microbiology, Immunology, and Molecular Genetics, UCLA School of Medicine, Los Angeles, CA 90095-1747. Phone: (310) 825-1982. Fax: (310) 206-1318. E-mail: uittenbo@ucla.edu.

† Present address: Genentech, 1 DNA Way, South San Francisco, CA 94080.

▽ Published ahead of print on 20 September 2006.

with delipidated bovine serum albumin (Sigma, St. Louis, MO) at 1,100 μg/ml, transferrin (Sigma, St. Louis, MO) at 85 μg/ml, and 2 mM glutamine and penicillin-streptomycin at 25 units/ml and 25 μg/ml, respectively (AT-IMDM) (27, 43). Purified, unconjugated murine monoclonal antibodies (mAb) to human CD45RA, CD27, CD69, and CD71 were obtained from Beckman Coulter (Miami, FL) and reconstituted in serum-free medium at 50 tests/μl for all but the CD27 mAb, which was reconstituted at 100 tests/μl. Fluorescence-conjugated mAb to CD3, CD4, CD8, CD27, CD45RA, CD69, and CD71 and isotype control antibodies of mouse immunoglobulin G1 (IgG1) and mouse IgG2 conjugated with fluorescein isothiocyanate (FITC), phycoerythrin (PE), and/or allophycocyanin (APC) were obtained from Becton Dickinson Immunocytometry Systems (BDIS; San Jose, CA). Monoclonal antibodies KC57-FITC and KC57-PE, which identify Gag_{HIV-1} antigens, were obtained from Beckman Coulter (Miami, FL). Monoclonal antibodies to CD3, CD4, and CD8 conjugated with Tricolor (Cy5-PE-tandem, referred to as Tricolor [TC]), mouse IgG2a-TC, and mAb to CD45RA conjugated to APC were obtained from Caltag (Burlingame, CA). Monoclonal antibodies to CCR5 (clone 2D7) and CXCR4 (clone 12G5) conjugated to FITC, PE, or APC were obtained from BD-Pharmingen (La Jolla, CA). 7-Amino-actinomycin D (7-AAD) and polyoxyethylene sorbitan monolaurate (Tween 20) were obtained from Sigma (St. Louis, MO). Paraformaldehyde was obtained from Polysciences, Inc. (Warrington, PA). Actinomycin D was obtained from Boehringer Mannheim (Indianapolis, IN).

Thymocyte preparation. Normal human postnatal thymus specimens were obtained from children undergoing corrective cardiac surgery. The tissue was placed in NH_4Cl-Tris lysing buffer to remove the red blood cells while the tissue was cut into small pieces and passed over a cell strainer to generate a single-cell suspension of thymocytes. The cells were washed in phosphate-buffered saline and serum-free medium (AT-IMDM). Thymocytes were resuspended at 2×10^7 cells/ml in serum-free medium for HIV-1 infection.

Immunomagnetic selection of thymocyte subsets. Goat anti-mouse M280 magnetic beads (6×10^9 to 7×10^9; Dynal, Lake Success, NY) were diluted to a 60-ml volume with serum-free medium without transferrin (A-IMDM) supplemented with 1% bovine serum albumin. The beads (1×10^8/ml) were coated with 25 μl of the following antibodies (50 tests/ml) overnight at 4°C: mouse anti-human CD45RA, mouse anti-human CD69, and mouse anti-human CD71. Thymocyte subsets were selected sequentially as described previously (27). Briefly, total thymocytes were incubated at a 1:1 ratio of CD45RA-coated M280 immunomagnetic beads to cells for 30 to 60 min at 4°C while rotating in a 15-ml culture tube in 4 to 5 ml medium. Cells were separated on a Dynal magnet, and both positively selected bead-bound cells and negatively selected $CD45RA^-$ thymocytes were collected for further rounds of selection. The $CD45RA^-$ population was incubated for 30 min at 4°C with 30 μl of CD27 mAb (100 tests/ml) in a 1-ml volume and then washed and incubated with M280 immunomagnetic beads at a 4:1 bead-to-cell ratio for 30 to 60 min at 4°C as described above. Both $CD27^+$ and $CD27^-$ fractions were collected. The resulting $CD45RA^-$ $CD27^-$ population was incubated with CD69-coated immunomagnetic beads at a 2:1 ratio as described above. CD69-positive and -negative fractions were collected. The resulting $CD45RA^-$ $CD27^-$ $CD69^-$ thymocyte population was incubated with CD71-coated M280 immunomagnetic beads at a bead-to-cell ratio of 1:1 for 30 to 60 min at 4°C while rotating and separated on a Dynal magnet into both positive and negative fractions. Each of the positively selected fractions was subjected to two more rounds of positive selection on the magnet to increase purity. Because the beads could not be removed for flow cytometric analysis of purity, we could only detect the purities of the negative fractions which were between 95 and 99%.

HIV-1 infection of SCID-hu mice and postnatal thymocytes. The syncytium-inducing, CXCR4-tropic hybrid molecular clone $HIV\text{-}1_{NL4\text{-}3}$ (NL4-3) was used for part of these studies (1). Virus stocks were prepared from daily harvests of supernatants from CEM cells (CCRF-CEM) infected with virus derived from COS cells electroporated with plasmid pNL4-3. Stocks of the non-syncytium-inducing, CCR5-tropic molecular clones $HIV\text{-}1_{JR\text{-}CSF}$ (JR-CSF) and $HIV\text{-}1_{NFN\text{-}SX}$ (NFN-SX) were prepared from 24-h harvests of supernatants from interleukin 2 (IL-2)- and phytohemagglutinin (PHA)-stimulated peripheral blood mononuclear cells infected with the supernatant of COS cells electroporated with plasmids pYKJR-CSF and pSX (22, 24). Virus stocks were stored at −70°C and treated with 2 μg/ml DNase (Worthington, Lakewood, N.J.) for 30 min at room temperature in the presence of 0.01 M $MgCl_2$ before infections. All infections were standardized by quantitating the infectious units in limiting-dilution studies using PHA-stimulated peripheral blood mononuclear cells (50, 51).

C.B.17 SCID mice were bred at UCLA and implanted with human fetal thymus and liver (thy/liv) grafts under the murine kidney capsule (2, 8). Four to 6 months postimplantation, the thy/liv grafts were infected by direct injection of HIV-1 into the graft. Ten nanograms of p24 from R5 $HIV\text{-}1_{JR\text{-}CSF}$ and 2 ng of p24 from X4 $HIV\text{-}1_{NL4\text{-}3}$ were injected into the implants in a 50-μl volume. Mock-infected implants, used as controls in all experiments, were prepared by injecting the implants with 50 μl of appropriate control supernatants. SCID-hu mice implanted with thy/liv grafts from the same donor were used for each individual experiment. The five different experiments included 6 to 27 SCID-hu mice per experiment, with 6 to 10 mice per time point. Thy/liv graft implants were taken between 1 and 9 weeks postinfection, and thymocytes were isolated as described above for the postnatal thymus specimens.

In vitro infection and culture of thymocytes were performed as previously described (27, 43). Briefly, 1×10^7 freshly isolated, nonstimulated thymocytes were incubated with 100 ng of X4 and R5 viral p24 in the presence of 10 μg/ml Polybrene (Sigma, St. Louis, MO) for 1 h at 37°C. Control thymocytes were mock infected in the presence of Polybrene with supernatants from the same uninfected cells used to prepare the virus stocks. After infection, the cells were washed, resuspended in serum-free medium, and cultured for 18 h.

Surface and intracellular immunophenotyping. Surface immunophenotyping of thymocytes with directly conjugated antibodies was performed as previously described (31, 32). Levels of CCR5 and CXCR4 expression in each subset were determined by gating on the following thymocyte populations: for subset IV, $CD45RA^+$ $CD3^+$ thymocytes; for subset III, $CD45RA^-$ $CD27^+$ $CD3^+$ thymocytes; for subset II, $CD27^-$ $CD69^+$ thymocytes; and for subset I, $CD69^-$ $CD3^-$ $CD71^+$ thymocytes.

Intracellular staining for Gag_{HIV-1} protein was performed after surface immunophenotyping and fixation in 1% paraformaldehyde. Fixed cells were subsequently permeabilized in 0.2% Tween 20 for 15 min at 37°C, washed with phosphate-buffered saline containing 2% newborn calf serum and 0.1% sodium azide (fluorescence-activated cell sorting [FACS] buffer), blocked with human AB serum, and stained with 2.5 μl KC57 fluorescent antibody or an IgG control. Finally, cells were washed with 0.2% Tween 20 and resuspended in FACS buffer before acquisition with a dual-laser FACSCalibur flow cytometer (BDIS, San Jose, CA). Multiparameter data acquisition and analysis were performed with Cell Quest software (BDIS).

Cell cycle analysis. Total human thymocytes were surface phenotyped using mAb conjugated to CD71-FITC and CD3-PE, fixed in 0.25% paraformaldehyde for 30 min, permeabilized by 0.2% Tween 20 for 15 min at 37°C, and incubated with 20 ng/ml of the DNA dye 7-amino-actinomycin D. Samples were acquired with a FACScan flow cytometer (BDIS, San Jose, CA). The FL3 area and FL3 width plot were displayed to gate out any aggregates with more then 4N DNA and subapoptotic cells with less then 2N DNA content. Data were analyzed using the cell cycle analysis software ModFit LT (from Verity Software House, Inc., Topsham, ME).

DNA isolation and PCR. DNA was isolated from in vitro-infected cultures at 18 h postinfection by phenol-chloroform extraction and ethanol precipitation as described previously (27). For samples collected from SCID-hu thymocyte subsets, simultaneous extraction of RNA and DNA was performed using TRIzol (Gibco/BRL-Life Technologies), following the manufacturer's protocol. Quantitative PCR was performed using an ABI Prism 7700 sequence detection system in a 25-μl reaction volume for 40 cycles between 95°C for 15 seconds and 60°C for 1 min, using the components in the TaqMan core reagent kit (Applied Biosystems, Foster City, CA). Proviral burden was measured using the primer pair SR1/AA55, which binds within the R and U5 regions of the long terminal repeat (LTR). This same pair was used to detect nucleotides synthesized at the initiation of reverse transcription. The SR1/661 primer pair spans the primer binding site and measures the completion of reverse transcription. The primers SR1 (5′-CAAGTAGTGTGTGCCCGTCTGT-3′), AA55 (5′-CTGCTAGAGATTTTCCACACTGAC-3′), and 661 (5′-CCTGCGTCGAGAGAGCTCCTCTGG-3′) were used along with the fluorogenic probe ZXF (5′-TGTGACTCTGGTAACTAGAGATCCCTCAGACCC-3′), modified with 6-carboxyfluorescein reporter dye on the 5′ end and 6-carboxytetramethylrhodamine quencher dye on the 3′ end. To control for the amount of cellular DNA per reaction, the following primers and probe were used to amplify a portion of the human beta-globin gene: forward primer BGF1 (5′-CAACCTCAAACAGACACCATGG-3′), reverse primer BGR1 (5′-TCCACGTTCACCTTGCCC-3′), and the fluorogenic probe modified as described above (5′-CTCCTGAGGAGAAGTCTGCCGTTACTGCC-3′).

Statistics. The Wilcoxon signed rank test was used to compare differences in HIV-1 entry, proviral burden, and levels of coreceptor expression for thymocytes at different stages of maturation. *P* values were adjusted for intracorrelation and intraexperiment correlations, where appropriate, through permutation methods. Due to small sample sizes, attention has been drawn to results that were significant at the 0.10 level or lower.

RESULTS

Delineation of distinct developmental stages of thymopoiesis. As T cells develop in the thymus, they receive developmental cues driving T-cell receptor (TCR) gene rearrangement, expression, and selection. These developmental stages are identified by the progressive expression of cell surface markers, leading to the eventual phenotype of naïve CD4 and CD8 single-positive T cells in the periphery (Fig. 1A). Using four-color flow cytometry, we immunophenotyped thymocytes with various combinations of the following activation/developmental stage markers: CD1, CD3, CD4, CD8, CD45RA, CD27, CD69, and CD71 (for our purposes indicated as stages I to IV and substage I-P). The most mature thymocytes at the last stage of thymopoiesis, about to emigrate from the thymus, express high levels of CD3 and the leukocyte common antigen CD45RA isoform (stage IV) (Fig. 1A). These mature CD45RA$^+$ CD3$^{+/hi}$ thymocytes express either CD4 or CD8 (16, 41, 44) (Fig. 1A). Thymocytes at the developmental stage preceding CD45RA expression (CD45RA$^-$ CD3$^{+/hi}$) express the tumor necrosis factor receptor family member CD27 (stage III) and include late CD4/CD8 double-positive cells as well as CD4 and CD8 single-positive cells (Fig. 1A). CD27 has been shown to function as a costimulatory molecule affecting the proliferation of peripheral T cells, which is consistent with CD27 expression in the thymus, where CD27 expression marks thymocytes that gain functional proliferative responsiveness to mitogens such as PHA (28, 46). The more immature population preceding CD3$^{+/low}$ CD45RA$^-$ CD27$^-$ cells (stage II) bears the activation marker CD69, a C-type lectin binding protein that arises in response to positive selection signaling for an appropriate TCR rearrangement (42). The most immature cells we examined were cells at the stage before positive-selection CD3$^-$ CD45RA$^-$ CD27$^-$ CD69$^-$ cells (stage I). Within this most immature stage, a subset of cells expresses the transferrin receptor CD71, also referred to as the proliferating antigen (stage I-P). In the thymus, the CD71$^+$ population is enriched in cells with more than 2N DNA as determined by flow cytometric measurements of DNA content by the DNA fluorescent molecule 7-amino-actinomycin D (Fig. 1B).

X4 and R5 HIV-1 replicate at distinct stages of thymopoiesis in vivo. To further delineate the stages of T-cell activation or development at which R5 and X4 HIV-1 replicate, thy/liv graft implants in SCID-hu mice were infected with X4 HIV-1 (NL4-3) (four experiments) or R5 HIV-1 (JR-CSF) (four experiments). Despite the rapid replication kinetics of NL4-3, virus expression was not detectable at 1 week postinfection in five out of five thy/liv grafts studied at that time point. At 19 days after infection with NL4-3, virus expression was detected by intracellular staining for Gag_{HIV-1} in two out of two thy/liv grafts at frequencies of 0.05 to 0.3% of the total thymocytes. At 4 and 5 weeks after infection with NL4-3, 6 out of 10 of the thy/liv graft implants expressed virus in 5 to 9% of the total thymocytes and depletion of CD4$^+$ and CD4$^+$ CD8$^+$ cells was observed. To detect JR-CSF expression, infected thy/liv graft implants were collected at weeks 1, 3.5, 4, 7, 8, and 9. No virus expression was detected at 1 week postinfection in five out of five JR-CSF-infected mice. However, 31 out of 33 thy/liv graft implants expressed JR-CSF after week 3.5 postinfection and the numbers of $Gag_{HIV-1}{}^+$ thymocytes ranged from 0.15 to 1.5% of the total population.

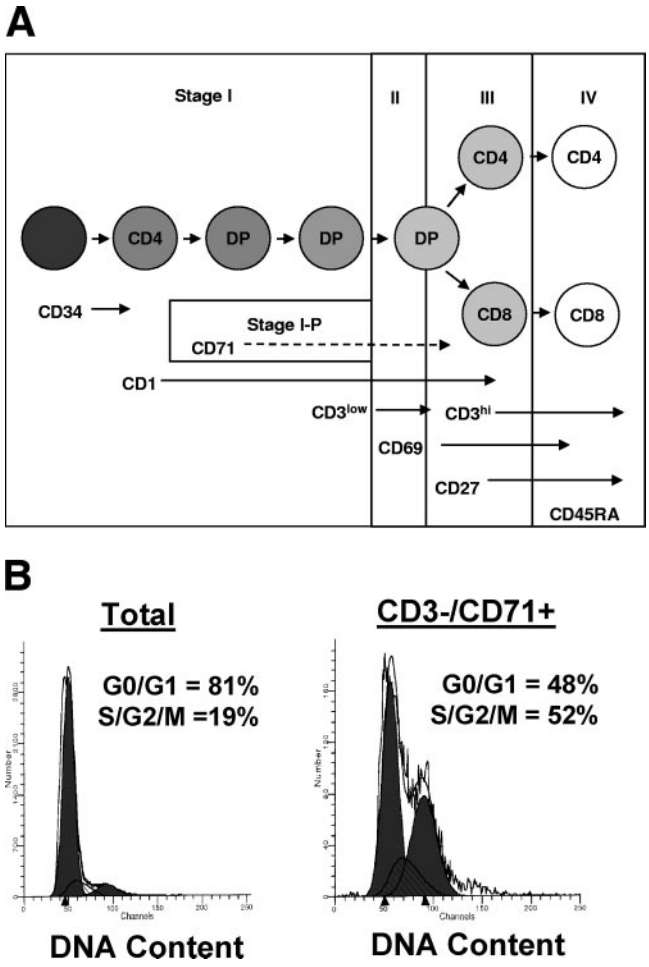

FIG. 1. Thymocyte development scheme. (A) Combinations of antibodies were used to identify thymocytes at five distinct stages of T-cell development. Stage I, CD69$^-$ thymocytes; stage I-P (a subset of stage I in which thymocytes express CD71), CD69$^-$ thymocytes; stage II, CD69$^+$ cells that have not yet acquired CD27 expression; stage III, CD69$^+$ CD27$^+$ thymocytes that have not yet acquired CD45RA expression; stage IV, CD27$^+$ thymocytes expressing CD45RA. Within stage I, the first circle represents the CD34$^+$ thymic immigrant. The second circle represents the immature CD4 single-positive thymocyte. The third and fourth circles represent CD3$^-$ CD4$^+$ CD8$^+$ double-positive (DP) thymocytes and CD3$^{+/low}$ DP thymocytes, respectively. The fifth circle (stages II/III) represents CD69$^+$ positively selected thymocytes in transition to the next stage of either CD4 single-positive or CD8 single-positive thymocytes. The last stage (stage IV) represents the CD3$^{+/hi}$ CD45RA$^+$ thymic emigrant. (B) Cell cycle analysis was determined for total and CD3$^-$ CD71$^+$ thymocytes by a combination of cell surface staining with antibodies to CD3 and CD71 and 7-AAD. Histograms were drawn for DNA content (7-AAD) in ungated thymocytes (left panel) and CD3$^-$ CD71$^+$ gated thymocytes (right panel). The proportions of the thymocytes in the G_0/G_1 stages and $S/G_2/M$ stages of the cell cycle were calculated by Modfit software.

By intracellular staining for Gag_{HIV-1} protein, we calculated the frequency of virus-expressing cells at each of the developmental stages of thymocyte maturation. In NL4-3-infected implants, more than 80% of the virus-expressing cells were present in the immature CD69$^-$ (stage I; CD3$^{-/low}$) popula-

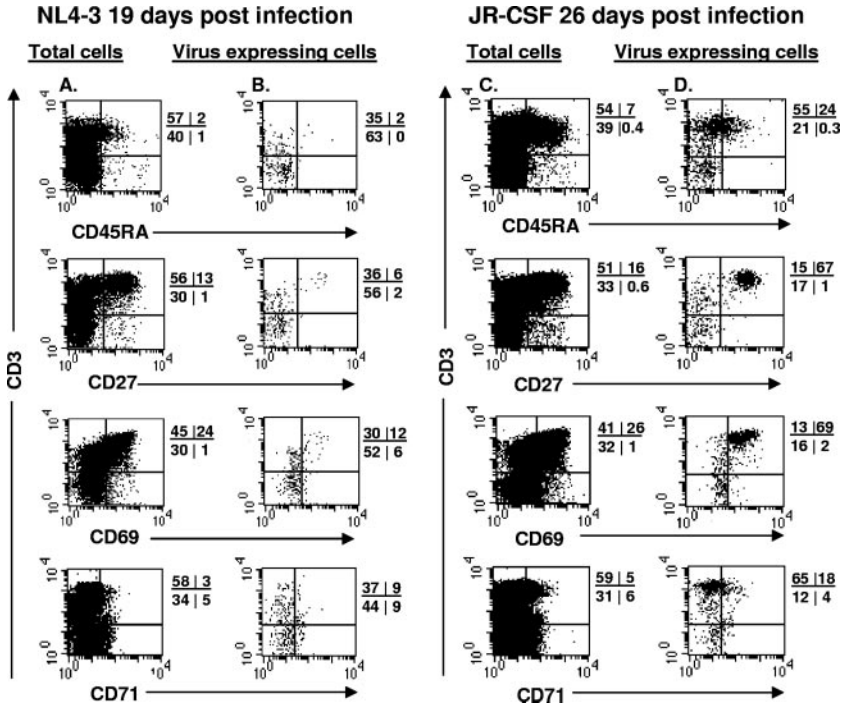

FIG. 2. X4 HIV-1 replicates in immature thymocytes, while R5 HIV-1 replicates in mature thymocytes in HIV-1-infected SCID-hu mice. Thymocytes were obtained from HIV-1-infected implants in SCID-hu mice at 19 days (NL4-3) and 26 days (JR-CSF) postinfection. The cells were surface stained with antibodies to CD3, CD71, CD69, CD27, and CD45RA combined with intracellular staining for Gag_{HIV-1} proteins (KC57-FITC). The phenotype of Gag_{HIV-1}-expressing cells was determined by gating on $KC57^+$ cells. The percentages of positive cells in each quadrant are indicated. Isotype controls were used to set the cursors. Results for one representative staining of two thymic implants at these time points are shown.

tion (Fig. 2). In contrast, in JR-CSF-infected SCID-hu mice, more than 70% of the virus-expressing thymocytes were mature $CD3^{+/hi}$ cells (Fig. 2). The majority of these mature JR-CSF-expressing thymocytes were $CD27^+$ and $CD69^+$, and 24% expressed CD45RA. Thus, at early time points after in vivo HIV-1 infection, X4 HIV-1 was expressed in very immature (stage I) thymocytes, while R5 HIV-1 was expressed mainly in mature (stage III) thymocytes.

Differences in R5 and X4 HIV-1 proviral burden in thymocyte subsets. To determine whether the differential expression of HIV-1 by X4 and R5 HIV-1 in thymocyte subsets was due to differences in the proviral levels or to a block in virus expression, we examined the HIV-1 DNA content in the thymocyte subsets by quantitative DNA PCR. At 4 and 7 weeks after infection of the thymic implant, we analyzed the R5 HIV-1-established infection in each of the thymocyte subsets. The proviral levels were calculated as numbers of copies per 100 cell equivalents as follows: for stage I-P, 10 ± 3.7; for stage I, 8.7 ± 2.8; for stage II, 5.1 ± 1.6; for stage III, 13.4 ± 3.8; for stage IV, 8.6 ± 0.7; and for the total population, 6.9 ± 2.5 (Fig. 3). These data indicate that proviral DNA was also high in immature thymocyte subsets. However, the R5 proviral burden in the stage III thymocyte subset was significantly higher ($P = 0.04$) than those in other subsets.

The average percentage of thymocytes expressing R5 Gag_{HIV-1}/cell (Table 1) was less than the average number of proviruses detected in this population (assuming one virus infection per cell in each subset) (Fig. 3), indicating that R5 HIV-1 persists through development in a nonexpressed form and is present as early as stage I-P (in the $CD3^-/CD71^+$ population). Dividing the percentage of cells expressing viral proteins (Table 1) by the percentage of provirus-harboring cells (Fig. 3), we found that the percentages of cells in each subset expressing R5 HIV-1 are as follows: for stage I-P, 12%; for stage I, 5.3%; for stage II, 17.8%; for stage III, 19.2%; and for stage IV, 26.7%.

As X4 HIV-1 causes substantial $CD4^+$ thymocyte depletion at weeks 4 to 7 postinfection, we chose to analyze X4 HIV-1 infection before T-cell loss occurs. We therefore determined the X4 proviral burden early, at 19 days postinfection. The proviral burdens, calculated as numbers of copies per 100 cell equivalents, were as follows: for subset I-P, 21.3 ± 9.8; for subset I, 8.5 ± 6.7; for subset II, 3.9 ± 3.5; for subset III, 2.3 ± 2.1; for subset IV, 1.1 ± 1.2; and for the total population, 0.5 ± 0.6. The X4 proviral burden in the stage I-P thymocyte subset was significantly higher ($P = 0.07$) than those in other subsets. We found that the subset producing most of the X4 virus also harbored the greatest proviral burden (Table 1 and Fig. 3).

Presumably, nonexpressed X4 HIV-1 is established at early developmental stages as well; however, with such rapid replication and CD4 thymocyte destruction in the X4 $HIV\text{-}1_{NL4\text{-}3}$-infected implant, not enough cells were available to select and purify each subset at late stages postinfection. Certainly, by 19 days postinfection, high X4 HIV-1 burden was achieved (Fig. 3), with barely detectable expression in the $CD3^-$ $CD71^+$ thymocyte subset (Table 1). Thus, all through thymocyte de-

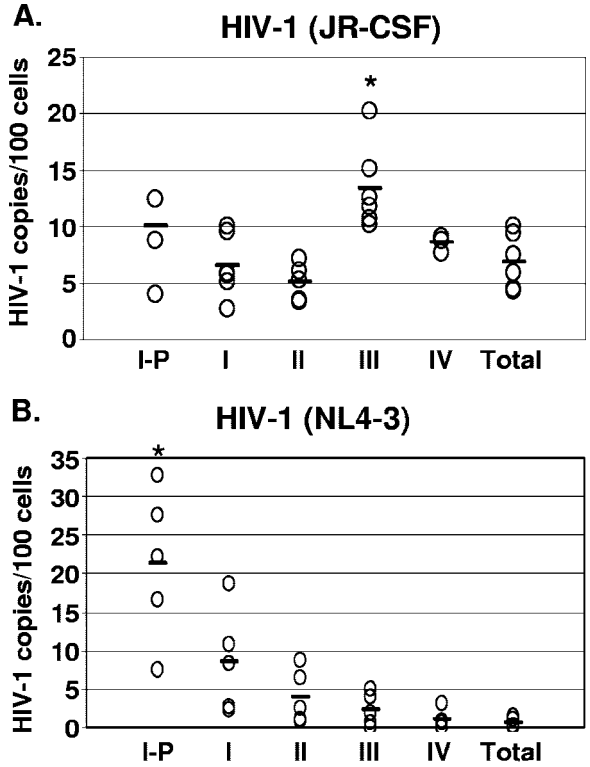

FIG. 3. R5 and X4 HIV-1 proviral burdens in thymocyte subsets at different stages of maturation. Thymocyte subsets were obtained from HIV-1-infected implants from SCID-hu mice by immunomagnetic bead selection. Quantitative TaqMan PCR for HIV-1 proviral burden relative to that of the human beta-globin gene was performed and calculated based on interpolation from standard curves. The level of HIV-1 per 100 cell equivalents for each implant in each subset is shown (open circles) (five to six data points in each subset). Asterisks indicate statistically significant differences. (A) Proviral burdens at 4 and 7 weeks postinfection (R5 HIV-1_{JR-CSF}-infected implants) and (B) at 19 days postinfection (X4 HIV-1_{NL4-3}).

velopment, cellular conditions may lead to a certain degree of nonexpressed R5 and X4 viral DNA or potentially latent HIV-1.

CCR5 and CXCR4 expression in distinct thymocyte subsets. Four-color flow cytometric analysis of CXCR4 and CCR5 expression was performed among the five stages of activation presented above to compare the relative levels of coreceptor expression within the thymocyte subsets. As we and others have described previously, the percentages of cells expressing CCR5 were low at all stages, with mature medullary thymocytes expressing the highest percentage of CCR5 (6, 26). We show more specifically that the greatest expression of CCR5 was present at stage III ($CD27^+$), with 2.5% ± 0.8% (Fig. 4). The percentage of CCR5 expression for stage III thymocytes was significantly higher ($P = 0.04$) than those for thymocytes at other stages of differentiation. In contrast, CXCR4 was expressed at high percentages in all thymocyte subsets. The highest levels of CXCR4 expression, as measured by mean fluorescent intensity, occurred on immature thymocytes and particularly on immature thymocytes at the cycling stage (stage I-P; $CD45RA^-$ $CD27^-$ $CD69^-$ $CD71^+$) (Fig. 4) (6, 20, 27). The level of CXCR4 expression on stage I-P thymocytes was significantly higher ($P = 0.07$) than those on thymocytes at other stages of differentiation. At the point of positive selection (stage II), CXCR4 was downregulated (39) (Fig. 4). Finally, prior to exiting the thymus, thymocytes demonstrated increased expression of CXCR4, and the frequency of CCR5 expression declined, generating the coreceptor levels found for peripheral blood naïve T cells (Fig. 4). Thus, differential levels of HIV-1 coreceptor expression were observed in thymocyte subsets at different stages of maturation. These patterns of coreceptor expression were found in all five postnatal thymus tissues examined.

HIV-1 entry in discrete thymocyte subsets correlates with levels of coreceptor expression. HIV-1 provirus was detected in all thymocyte subsets tested, yet the virus may have entered at an earlier developmental stage. Therefore, to examine the susceptibility of each of the thymocyte subsets to direct HIV-1 infection, we purified each of the five subsets (stages I-P and I to IV) and infected each subset in vitro. The role of Env for conferring the chemokine receptor tropism of a virus was examined by infection of thymocyte subsets with R5 HIV-1_{NFN-SX}, derived from NL4-3, with only 157 amino acid differences in the Env protein (24). Each of the thymocyte subsets was infected in parallel with X4 HIV-1_{NL4-3}, R5 HIV-1_{NFN-SX}, and R5 HIV-1_{JR-CSF} in vitro for 18 h. As we and others described previously, X4 entry was greater than R5 entry in the thymocyte subsets due to the greater prevalence of CXCR4 expression than CCR5 expression in thymocytes (6, 27). Viral entry of R5 HIV-1 (NFN-SX and JR-CSF) was highest in the $CD27^+$ $CD45RA^-$ thymocyte subset in three out of three experiments in which cells were infected with equal amounts of virus (Fig. 5). The mean viral-copy numbers of NFN-SX and JR-CSF

TABLE 1. Frequencies of X4 HIV-1 (NL4-3) and R5 HIV-1 (JR-CSF) expression in thymocyte subsets in SCID-hu mice[a]

Virus	Wk	Frequency of virus expression in indicated thymocyte subset				
		Subset I-P	Subset I	Subset II	Subset III	Subset IV
X4 HIV-1 (NL4-3)	2.5	0.08	0.04	0.03	0.02	0.01
	2.5	0.6	0.3	0.13	0.16	0.2
	4	28.8	18.2	5.4	5	5.5
	4	27.5	17.9	4.3	5.3	6.5
	4	24.8	18.8	5.3	7.2	8.7
	5	26	18.8	24	ND	1.5
	5	23	10.7	4.5	ND	4.5
R5 HIV-1 (JR-CSF)	3.5	0.5	0.3	0.4	3.1	2
	3.5	0.6	0.3	0.4	2.4	5.1
	4	0.5	0.3	0.6	2.7	2.7
	4	0.7	0.6	1.1	3.1	3.6
	4	0.5	0.6	1.0	2.7	2.3
	4	0.7	0.2	0.4	2.6	2.4
	4	1.2	0.2	0.3	2.2	2.1
	4	2.3	0.3	1	2	1.4
	7	1.0	0.5	1.1	ND	1.1
	7	2.1	0.9	2.3	ND	1.6
	7	3.2	1.1	1.4	ND	1.3
	7	0.4	0.2	0.6	ND	1.8

[a] Thymocytes were isolated from HIV-1-infected implants from 2.5 to 7 weeks postinfection. The cells were surface stained with antibodies to CD3, CD71, CD69, CD27, and CD45RA combined with intracellular staining for the Gag_{HIV-1} protein (KC57-FITC). Each specific subset was gated electronically, and the frequencies of Gag_{HIV-1} ($KC57^+$)-expressing cells in the subsets were determined. ND, not determined.

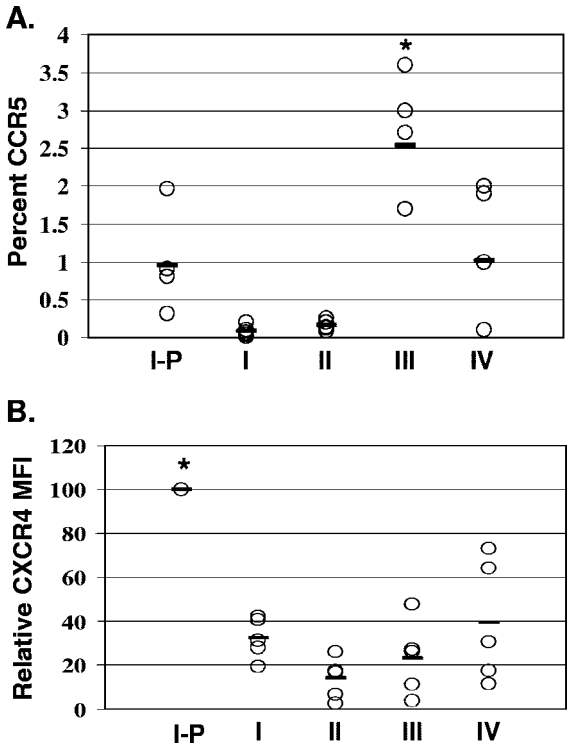

FIG. 4. HIV-1 coreceptor expression in thymocytes at five developmental stages. CCR5 and CXCR4 expression at stages I-P to IV of thymocyte development was determined by four-color flow cytometric analysis using combinations of monoclonal antibodies to CCR5-PE, CXCR4-PE, CD3-FITC and -APC, CD45RA-APC, CD27-FITC, CD69-TC, and CD71-FITC in five separate experiments as described in Materials and Methods. Asterisks indicate statistically significant differences. As only small numbers of thymocytes express CCR5 and almost all thymocytes express CXCR4, CCR5 data are expressed in percentages and CXCR4 data as mean fluorescence intensities. (A) The mean percent $CCR5^+$ cells in each subset was as follows: for subset I-P, 0.95% ± 0.6%; for subset I, 0.08% ± 0.07%; for subset II, 0.16% ± 0.06%; for subset III, 2.5% ± 0.8%; and for subset IV, 1% ± 0.9%. (B) Since CXCR4 is expressed in each of these subsets, we measured the mean fluorescent intensity (or geometric mean) of CXCR4 for each subset relative to that for subset I-P, which consistently expressed the highest levels of CXCR4 in all five experiments. Subset I-P, 100%; subset I, 32% ± 9%; subset II, 14% ± 9%; subset III, 23% ± 17%; and subset IV, 39% ± 28%.

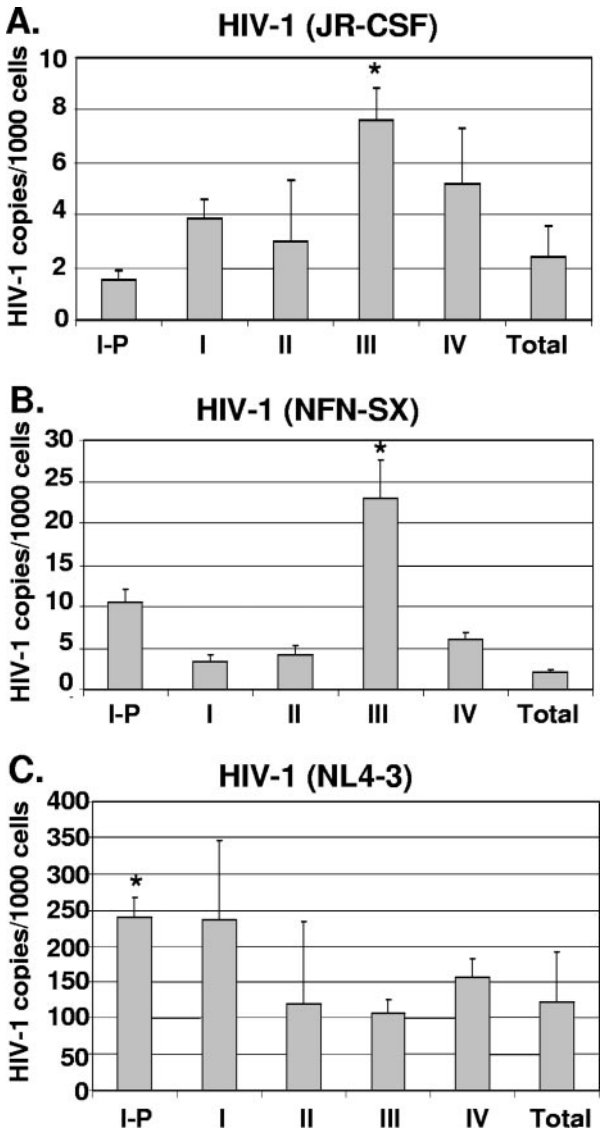

FIG. 5. HIV-1 entry in thymocyte subsets at different stages of maturation. Postnatal thymocytes were separated into individual subsets by magnetic beads and infected in vitro. Eighteen hours postinfection, quantitative PCR was performed to measure the number of initial reverse transcription products (R-U5), and the cell numbers were determined by beta-globin quantitative PCR. Values were calculated based on interpolation from a standard curve, and HIV-1 copy numbers were normalized to 1,000-cell equivalents from each subset after infection by R5 $HIV\text{-}1_{JR\text{-}CSF}$ (A), R5 $HIV\text{-}1_{NFN\text{-}SX}$ (B), and X4 $HIV\text{-}1_{NL4\text{-}3}$ (C). The mean viral-copy numbers and standard deviations for X4 and R5 HIV-1 DNA based on triplicate measurements in one representative experiment out of three are shown. Asterisks indicate statistically significant differences calculated based on data from three independent experiments.

DNA per 1,000 cells were as follows, respectively: for the total thymocytes, 2 and 2.4; for stage I-P, 10.5 and 1.5; for stage I, 3.3 and 3.9; for stage II, 4.2 and 3; for stage III ($CD27^+$), 23 and 7.6; and for stage IV, 6 and 5.2. These data indicate that R5 HIV-1 viral entry was 2- to 12-fold higher in $CD27^+$ cells than in the total population after in vitro infection (Fig. 5A and B). R5 $HIV\text{-}1_{NFN\text{-}SX}$ entry was statistically significantly higher in stage III thymocytes ($P = 0.02$) than in other subsets, while $HIV\text{-}1_{JR\text{-}CSF}$ entry in stage III thymocytes reached statistical significance ($P = 0.09$). R5 $HIV\text{-}1_{JR\text{-}CSF}$ entry was dependent on the presence of CCR5 since entry was prevented by the CCR5 antagonist TAK779 (3) (data not shown). X4 HIV-1 entry was quite efficient among all thymocyte subsets but was significantly higher in stage I-P thymocytes ($P = 0.01$) than in other subsets. Thus, X4 and R5 HIV-1 entered thymocyte subsets at all stages of differentiation. However, while R5 entry occurred in all subsets, the highest level of R5 entry was observed in the $CD27^+$ $CD45RA^-$ developmental stage (stage III).

Each thymocyte subset is sufficiently active for R5 and X4 HIV-1 reverse transcription. As reported for peripheral quiescent T cells, the completion of reverse transcription is dependent on the activation state of the cell (21). By harvesting

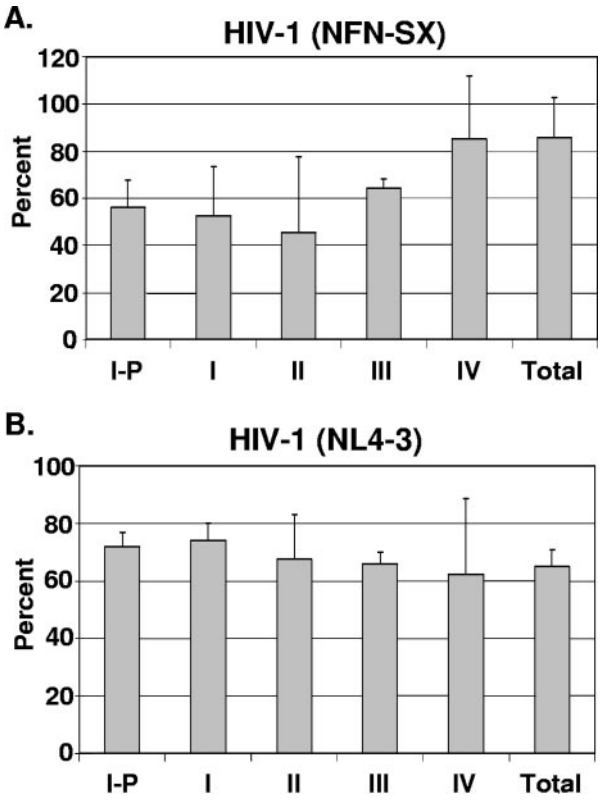

FIG. 6. Levels of HIV-1 reverse transcription are similar in thymocyte subsets at different stages of maturation. Postnatal thymocytes were separated into individual subsets by magnetic beads and infected in vitro. Eighteen hours postinfection, quantitative PCR was performed to measure the numbers of initial and full reverse transcription products (R-U5) and full reverse transcripts only (LTR-gag). The percent completion of reverse transcription for each subset was calculated by dividing the number of full-length transcripts by the number of total transcripts (initial and full). Values were calculated based on interpolation from a standard curve. (A) R5 HIV-1_{NFN-SX}-infected thymocytes. (B) X4 HIV-1_{NL4-3}-infected thymocytes. The means and standard deviations for triplicate measurements from one representative experiment out of three are shown.

the thymocyte subsets within 24 h postinfection, we sought to investigate the process of reverse transcription by DNA PCR within the first round of infection. Primers spanning the primer binding site (LTR to *gag*) were used to amplify proviral DNA species that have completed reverse transcription, and the amount of the product was compared to the amplified signal from the R-U5 (initiation) primer pair. The data shown in Fig. 6 are representative of three experiments showing equal efficiencies for reverse transcription of X4 HIV-1_{NL4-3} as well as R5 HIV-1_{NFN-SX} in each of the subsets tested. Thus, R5 and X4 HIV-1 reverse transcription took place at similar levels in all thymocyte subsets at different stages of maturation despite the differences observed in viral entry and expression.

DISCUSSION

Upon examining HIV-1 replication in thymocyte subsets associated with markers of activation, we found for the first time preferential entry and replication of R5 HIV-1 more specifically in $CD3^{+/hi}$ $CD27^{+}$ thymocytes in vivo in the SCID-hu model. This finding has important implications for HIV-1 pathogenesis, as thymocytes acquire functional capabilities at the $CD3^{+/hi}$ $CD27^{+}$ $CD1^{-}$ stage of development (28). Thus, despite the relatively low levels of viral replication and depletion of $CD4^{+}$ thymocytes after R5 HIV-1 infection, infection of a functionally important subset can potentially severely impact the regeneration of functional T cells in the periphery. We further show that the highest level of X4 HIV-1 expression occurred in the immature $CXCR4^{+/hi}$ $CD3^{-}$ $CD71^{+}$ proliferating thymocytes at early time points after infection. These data are in agreement with previous reports that R5 HIV-1 replicates in the mature thymocytes in the medulla (5, 20, 29) and X4 HIV-1 replicates in the immature, $CXCR4^{+/hi}$ thymocytes in the cortex of the thymus but further delineates the precise stage of thymopoiesis for R5 and X4 HIV-1 targets.

The $CD3^{+/hi}$ $CD27^{+}$ $CD1^{-}$ thymocyte subset marks cells that have received signals through the T-cell receptor to drive positive selection of the $CD4^{+}$ $CD8^{+}$ thymocytes and have acquired functional responsiveness (28). Thus, after positive selection, CXCR4 expression decreases and CCR5 expression increases. This is also the stage where thymocytes respond to the cytokines IL-2 and IL-4 to produce high levels of HIV-1 in vitro (26). This process of decreased CXCR4 and increased CCR5 expression after T-cell receptor signaling in the thymus mirrors an occurrence in the periphery, where CXCR4 expression decreases and CCR5 expression increases as naïve cells progress to memory cells (7). In addition, functional responsiveness to antigen is improved in the memory cells compared to that in the naïve T cells, just as functional responsiveness to mitogens is acquired in the positively selected thymocytes (28).

Despite the low level of CCR5 expression, we found that R5 viruses could infect and replicate in all the subsets tested. In agreement with our results, Scoggins et al. showed that even a more cytopathic R5 HIV-1 isolate persisted in using exclusively CCR5 in the SCID-hu model (35). As predicted by CXCR4 expression, X4 viruses also entered all the subsets tested; however, the greatest viral burden and highest frequency of expression were observed in the $CD3^{-}$ $CD71^{+}$ subset. Consistent with CD71, the transferrin receptor, which is referred to as the proliferation antigen, we found about 50% of the $CD71^{+}$ cells well into the S/G_2 and M phases of the cell cycle, whereas only 20% of the total population was beyond the G_1 phase of the cell cycle. Thus, part of the enhanced cytopathicity of X4 viruses in the thymus may be due not only to direct cell depletion but also to the destruction of the replicative capacity of early thymocytes. Camerini et al. calculated a proviral load of one provirus for 11 cells as a threshold for $CD4^{+}$ thymocyte depletion in the SCID-hu mouse model (10). By our measurements, X4 HIV-1_{NL4-3} achieved this threshold in immature thymocytes at the $CD3^{-}$ $CD71^{+}$ stage (stage I-P) as early as 19 days postinfection, while R5 HIV-1 reached this threshold at the mature $CD3^{+/hi}$ $CD27^{+}$ stage (stage III).

We also show that human thymocytes at multiple stages of development are permissible for direct HIV-1 entry and reverse transcription in vitro. Though quiescent peripheral T lymphocytes render HIV-1 unable to complete reverse transcription in vitro (50), we found that thymocyte subsets at numerous developmental stages are sufficiently activated for HIV-1 to complete reverse transcription in vitro. Factors such as TCR signal strength and IL-2 signaling of resting peripheral

T cells are needed for HIV-1 infection to pass the reverse transcription stage (25). Thymocytes may therefore receive sufficient signals by endogenous cytokines or TCR engagement for completion of reverse transcription to take place. Alternatively, Korin and Zack indicated that completion of reverse transcription was dependent on peripheral T cells at or beyond the G_1b phase of the cell cycle (21). Though we did not determine the cell cycle stages of the various thymocyte subsets, we did not observe any limitations in the reverse transcription process for any of the subsets tested. However, a block in vitro may not correlate with a block in vivo, for Eckstein et al. showed that in vitro nonproductively infected naïve quiescent T cells are productively infected when residing in the microenvironment of the lymph nodes in vivo (13). Thus, HIV-1 replication in distinct thymocyte subsets correlates more with coreceptor expression than with the activation state of thymocytes.

Human thymocytes appear permissible to HIV-1 replication by well-characterized molecular clones NL4-3 and JR-CSF. However, Stoddart et al. reported that protease inhibitor-resistant isolates are not propagated in the SCID-hu thymus despite sufficient replication in peripheral T cells (38). The mechanism for this thymocyte-selective block in HIV-1 replication is unknown, but it does raise the question as to how well molecularly disparate quasi-species present in vivo are able to replicate in the thymus. We previously measured and compared the replicative capacities of 10 HIV-1 isolates from children to those of the well-characterized X4 HIV-1_{NL4-3} and R5 HIV-1_{JR-CSF} clones in vitro (26). R5 HIV-1 isolates prevailed over X4 isolates among these pediatric isolates, which were obtained as close to birth as possible. We found that X4 primary isolates were not more cytopathic for thymocytes than the R5 isolates, indicating that coreceptor use by HIV-1 primary isolates was important but not the sole determinant of HIV-1 pathogenesis in the thymus (26). These data are supported by the finding that replication in $CD4^+$ T-cell cultures of R5 HIV-1 isolates is higher than that in X4 and dual tropic HIV-1 isolates (34). Camerini et al. reported that the determinants for cytopathicity were due to replication levels, and X4 Env enabled greater entry and replication than R5 HIV-1 in the thymus, reaching the critical threshold of replication for cytopathic effects (10).

Brooks et al. proposed that X4 HIV-1 latency in peripheral T cells could be established after infection of the thymus by using the SCID-hu mouse model (9). Latency formation is attributed to a decrease in viral transcription as thymocytes mature. In agreement with this, we found that the frequencies of X4-expressing cells decreased within progressively maturing thymocyte subsets. However, with R5 HIV-1, we found that the frequencies of R5 virus expression and proviral burden increased in thymocytes at more-mature stages of development (stages III and IV). Although R5 HIV-1 replication frequency increased in the mature subsets, at stages III and IV, where 2 to 5% of the cells expressed HIV-1, the proviral burdens ranged from 8 to 20% (on average, greater than 80% of R5 HIV-1-infected thymocytes did not express HIV-1), thereby confirming the notion that a pool of potentially latently infected cells is likely exported to the periphery. Even at the early (I and I-P) stages of thymopoiesis, R5 HIV-1 expression occurred in 0.3 to 3% of thymocytes, whereas the proviral burdens ranged from 10 to 28% of thymocytes in stages I and I-P, indicating that latency can be potentially established early in development and maintained throughout thymocyte development. Thus, thymocytes at multiple stages of development are permissive for viral replication and are at an optimal activation state for viral entry, reverse transcription, and latency formation.

Our results were obtained with the SCID-hu mouse model, which allows access to, and dissection of, thymocyte subsets for extensive ex vivo analysis of R5 and X4 HIV-1 infection in thymocyte subsets. The model was the first to correctly show that *nef* deletion results in attenuated HIV-1 replication, that breakthrough of HIV-1 replication can occur in vivo in the face of antiretroviral therapy, and that the thymus is not permanently damaged by HIV-1 replication (reviewed in reference 19). These findings have consistently shown that the SCID-hu mouse model accurately recapitulates HIV-1 pathogenesis in humans. There are certainly limitations to the model, such as a lack of immune responses and an absence of peripheral lymphoid cells (19). However, the SCID-hu mouse model does allow for an accurate assessment of the impact of HIV-1 on the development and regeneration of naïve T cells.

ACKNOWLEDGMENTS

This work was supported by the National Institutes of Health (AI 54286, AI 52833, and UCLA CFAR).

We thank Hillel Laks and his colleagues and staff for providing us with the thymus specimens, John Boscardin for performing the statistical analysis of the data, Deborah Anisman-Posner and Silvia Neagos for their excellent technical assistance, and Beth Jamieson, Susan Plaeger, Paul Krogstad, Otto Yang, and Arnaud Colantonio for helpful discussions and critical review of the manuscript.

REFERENCES

1. **Adachi, A., H. E. Gendelman, S. Koenig, T. Folks, R. Willey, A. Rabson, and M. A. Martin.** 1986. Production of acquired immunodeficiency syndrome-associated retrovirus in human and nonhuman cells transfected with an infectious molecular clone. J. Virol. **59:**284–291.
2. **Aldrovandi, G. M., G. Feuer, L. Gao, B. Jamieson, M. Kristeva, I. S. Y. Chen, and J. A. Zack.** 1993. The SCID-hu mouse as a model for HIV-1 infection. Nature **363:**732–736.
3. **Baba, M., O. Nishimura, N. Kanzaki, M. Okamoto, H. Sawada, Y. Iizawa, M. Shiraishi, Y. Aramaki, K. Okonogi, Y. Ogawa, K. Meguro, and M. Fujino.** 1999. A small-molecule, nonpeptide CCR5 antagonist with highly potent and selective anti-HIV-1 activity. Proc. Natl. Acad. Sci. USA **96:**5698–5703.
4. **Bakri, Y., C. Schiffer, V. Zennou, P. Charneau, E. Kahn, A. Benjouad, J. C. Gluckman, and B. Canque.** 2001. The maturation of dendritic cells results in postintegration inhibition of HIV-1 replication. J. Immunol. **166:**3780–3788.
5. **Berkowitz, R. D., S. Alexander, C. Bare, V. Linquist-Stepps, M. Bogan, M. E. Moreno, L. Gibson, E. D. Wieder, J. Kosek, C. A. Stoddart, and J. M. McCune.** 1998. CCR5- and CXCR4-utilizing strains of human immunodeficiency virus type 1 exhibit differential tropism and pathogenesis in vivo. J. Virol. **72:**10108–10117.
6. **Berkowitz, R. D., K. P. Beckerman, T. J. Schall, and J. M. McCune.** 1998. CXCR4 and CCR5 expression delineates targets for HIV-1 disruption of T cell differentiation. J. Immunol. **161:**3702–3710.
7. **Bleul, C. C., L. Wu, J. A. Hoxie, T. A. Springer, and C. R. Mackay.** 1997. The HIV coreceptors CXCR4 and CCR5 are differentially expressed and regulated on human T lymphocytes. Proc. Natl. Acad. Sci. USA **94:**1925–1930.
8. **Bonyhadi, M. L., L. Rabin, S. Salimi, D. A. Brown, J. Kosek, J. M. McCune, and H. Kaneshima.** 1993. HIV induces thymus depletion in vivo. Nature **363:**728–732.
9. **Brooks, D. G., S. G. Kitchen, C. M. Kitchen, D. D. Scripture-Adams, and J. A. Zack.** 2001. Generation of HIV latency during thymopoiesis. Nat. Med. **7:**459–464.
10. **Camerini, D., H. P. Su, G. Gamez-Torre, M. L. Johnson, J. A. Zack, and I. S. Chen.** 2000. Human immunodeficiency virus type 1 pathogenesis in SCID-hu mice correlates with syncytium-inducing phenotype and viral replication. J. Virol. **74:**3196–3204.
11. **Deng, H., R. Liu, W. Ellmeier, S. Choe, D. Unutmaz, M. Burkhart, P. DiMarzio, S. Marmon, R. E. Sutton, C. M. Hill, C. B. Davis, S. C. Peiper,**

T. J. Schall, D. Littman, and N. R. Landau. 1996. Identification of a major co-receptor for primary isolates of HIV-1. Nature **381:**661–666.
12. **Dragic, T., V. Litwin, G. P. Allaway, S. R. Martin, Y. Huang, K. A. Nagashima, C. Cayanan, P. J. Maddon, R. A. Koup, J. P. Moore, and W. A. Paxton.** 1996. HIV-1 entry into CD4$^+$ cells is mediated by the chemokine receptor CC-CKR5. Nature **381:**667–672.
13. **Eckstein, D. A., M. L. Penn, Y. D. Korin, D. D. Scripture-Adams, J. A. Zack, J. F. Kreisberg, M. Roederer, M. P. Sherman, P. S. Chin, and M. A. Goldsmith.** 2001. HIV-1 actively replicates in naive CD4(+) T cells residing within human lymphoid tissues. Immunity **15:**671–682.
14. **Fais, S., C. Lapenta, S. M. Santini, M. Spada, S. Parlato, M. Logozzi, P. Rizza, and F. Belardelli.** 1999. Human immunodeficiency virus type 1 strains R5 and X4 induce different pathogenic effects in hu-PBL-SCID mice, depending on the state of activation/differentiation of human target cells at the time of primary infection. J. Virol. **73:**6453–6459.
15. **Feng, Y., C. C. Broder, P. E. Kennedy, and E. A. Berger.** 1996. HIV-1 entry cofactor: functional cDNA cloning of a seven-transmembrane, G protein-coupled receptor. Science **272:**872–877.
16. **Fujii, Y., M. Okumura, K. Inada, K. Nakahara, and H. Matsuda.** 1992. CD45 isoform expression during T cell development in the thymus. Eur. J. Immunol. **22:**1843–1850.
17. **Ho Tsong Fang, R., E. Khatissian, V. Monceaux, M. C. Cumont, S. Beq, J. C. Ameisen, A. M. Aubertin, N. Israel, J. Estaquier, and B. Hurtrel.** 2005. Disease progression in macaques with low SIV replication levels: on the relevance of TREC counts. AIDS **19:**663–673.
18. **Jamieson, B. D., S. Pang, G. M. Aldrovandi, J. Zha, and J. A. Zack.** 1995. In vivo pathogenic properties of two clonal HIV-1 isolates. J. Virol. **69:**6259–6264.
19. **Jamieson, B. D., and J. A. Zack.** 1999. Murine models for HIV disease. AIDS **13**(Suppl. A)**:**S5–S11.
20. **Kitchen, S. G., and J. A. Zack.** 1997. CXCR4 expression during lymphopoiesis: implications for human immunodeficiency virus type 1 infection of the thymus. J. Virol. **71:**6928–6934.
21. **Korin, Y. D., and J. A. Zack.** 1998. Progression to the G_1b phase of the cell cycle is required for completion of human immunodeficiency virus type 1 reverse transcription in T cells. J. Virol. **72:**3161–3168.
22. **Koyanagi, Y., S. Miles, R. T. Mitsuyasu, J. E. Merill, H. V. Vinters, and I. S. Y. Chen.** 1987. Dual infection of the central nervous system by AIDS viruses with distinct cellular tropisms. Science **236:**819–822.
23. **Lawn, S. D., S. T. Butera, and T. M. Folks.** 2001. Contribution of immune activation to the pathogenesis and transmission of human immunodeficiency virus type 1 infection. Clin. Microbiol. Rev. **14:**753–777.
24. **O'Brien, W. A., Y. Koyanagi, A. Namazie, J. Q. Zhao, A. Diagne, K. Idler, J. A. Zack, and I. S. Chen.** 1990. HIV-1 tropism for mononuclear phagocytes can be determined by regions of gp120 outside the CD4-binding domain. Nature **348:**69–73.
25. **Oswald-Richter, K., S. M. Grill, M. Leelawong, and D. Unutmaz.** 2004. HIV infection of primary human T cells is determined by tunable thresholds of T cell activation. Eur. J. Immunol. **34:**1705–1714.
26. **Pedroza-Martins, L., W. J. Boscardin, D. J. Anisman, D. Schols, Y. J. Bryson, and C. H. Uittenbogaart.** 2002. Impact of cytokines on replication in the thymus of primary human immunodeficiency virus type 1 isolates from infants. J. Virol. **76:**6929–6943.
27. **Pedroza-Martins, L., K. B. Gurney, B. E. Torbett, and C. H. Uittenbogaart.** 1998. Differential tropism and replication kinetics of human immunodeficiency virus type 1 isolates in thymocytes: coreceptor expression allows viral entry, but productive infection of distinct subsets is determined at the postentry level. J. Virol. **72:**9441–9452.
28. **Res, P., B. Blom, T. Hori, K. Weijer, and H. Spits.** 1997. Downregulation of CD1 marks acquisition of functional maturation of human thymocytes and defines a control point in late stages of human T cell development. J. Exp. Med. **185:**141–151.
29. **Reyes, R. A., D. R. Canfield, U. Esser, L. A. Adamson, C. R. Brown, C. Cheng-Mayer, M. B. Gardner, J. M. Harouse, and P. A. Luciw.** 2004. Induction of simian AIDS in infant rhesus macaques infected with CCR5- or CXCR4-utilizing simian-human immunodeficiency viruses is associated with distinct lesions of the thymus. J. Virol. **78:**2121–2130.
30. **Rosenzweig, M., M. Connole, A. Forand-Barabasz, M. P. Tremblay, R. P. Johnson, and A. A. Lackner.** 2000. Mechanisms associated with thymocyte apoptosis induced by simian immunodeficiency virus. J. Immunol. **165:**3461–3468.
31. **Schmid, I., W. J. Krall, C. H. Uittenbogaart, J. Braun, and J. V. Giorgi.** 1992. Dead cell discrimination with 7-amino-actinomycin D in combination with dual color immunofluorescence in single laser flow cytometry. Cytometry **13:**204–208.
32. **Schmid, I., C. H. Uittenbogaart, and J. V. Giorgi.** 1991. A gentle fixation and permeabilization method for combined cell surface and intracellular staining with improved precision in DNA quantification. Cytometry **12:**279–285.
33. **Schmidtmayerova, H., M. Alfano, G. Nuovo, and M. Bukrinsky.** 1998. Human immunodeficiency virus type 1 T-lymphotropic strains enter macrophages via a CD4- and CXCR4-mediated pathway: replication is restricted at a postentry level. J. Virol. **72:**4633–4642.
34. **Schweighardt, B., A. M. Roy, D. A. Meiklejohn, E. J. Grace II, W. J. Moretto, J. J. Heymann, and D. F. Nixon.** 2004. R5 human immunodeficiency virus type 1 (HIV-1) replicates more efficiently in primary CD4$^+$ T-cell cultures than X4 HIV-1. J. Virol. **78:**9164–9173.
35. **Scoggins, R. M., J. R. Taylor, Jr., J. Patrie, A. B. van't Wout, H. Schuitemaker, and D. Camerini.** 2000. Pathogenesis of primary R5 human immunodeficiency virus type 1 clones in SCID-hu mice. J. Virol. **74:**3205–3216.
36. **Sopper, S., D. Nierwetberg, A. Halbach, U. Sauer, C. Scheller, C. Stahl-Hennig, K. Matz-Rensing, F. Schafer, T. Schneider, V. ter Meulen, and J. G. Muller.** 2003. Impact of simian immunodeficiency virus (SIV) infection on lymphocyte numbers and T-cell turnover in different organs of rhesus monkeys. Blood **101:**1213–1219.
37. **Spits, H.** 2002. Development of alphabeta t cells in the human thymus. Nat. Rev. Immunol. **2:**760–772.
38. **Stoddart, C. A., T. J. Liegler, F. Mammano, V. D. Linguist-Stepps, M. S. Hayden, S. G. Deeks, R. M. Grant, F. Clavel, and J. M. McCune.** 2001. Impaired replication of protease inhibitor-resistant HIV-1 in human thymus. Nat. Med. **7:**712–718.
39. **Suzuki, G., Y. Nakata, Y. Dan, A. Uzawa, K. Nakagawa, T. Saito, K. Mita, and T. Shirasawa.** 1998. Loss of SDF-1 receptor expression during positive selection in the thymus. Int. Immunol. **10:**1049–1056.
40. **Taylor, J. R., Jr., K. C. Kimbrell, R. Scoggins, M. Delaney, L. Wu, and D. Camerini.** 2001. Expression and function of chemokine receptors on human thymocytes: implications for infection by human immunodeficiency virus type 1. J. Virol. **75:**8752–8760.
41. **Tedder, T. F., L. C. Clement, and M. D. Cooper.** 1985. Human lymphocyte differentiation antigens HB-10 and HB-11. I. Ontogeny of antigen expression. J. Immunol. **134:**2983–2988.
42. **Testi, R., J. H. Phillips, and L. L. Lanier.** 1988. Constitutive expression of a phosphorylated activation antigen (Leu 23) by CD3^{bright} human thymocytes. J. Immunol. **141:**2557–2563.
43. **Uittenbogaart, C. H., D. J. Anisman, J. A. Zack, A. Economides, I. Schmid, and E. F. Hays.** 1995. Effects of cytokines on HIV-1 production by thymocytes. Thymus **23:**155–175.
44. **Uittenbogaart, C. H., S. Higashitani, I. Schmid, L. W. Vollger, T. Boone, and L. T. Clement.** 1990. Interleukin-4 induces expression of the CD45RA antigen on human thymocyte subpopulations. Int. Immunol. **2:**1179–1187.
45. **Unutmaz, D.** 2001. T cell signaling mechanisms that regulate HIV-1 infection. Immunol. Res. **23:**167–177.
46. **Vanhecke, D., B. Verhasselt, M. De Smedt, G. Leclercq, J. Plum, and B. Vandekerckhove.** 1997. Human thymocytes become lineage committed at an early postselection CD69+ stage, before the onset of functional maturation. J. Immunol. **159:**5973–5983.
47. **Vicenzi, E., P. P. Bordignon, P. Biswas, A. Brambilla, C. Bovolenta, M. Cota, F. Sinigaglia, and G. Poli.** 1999. Envelope-dependent restriction of human immunodeficiency virus type 1 spreading in CD4$^+$ T lymphocytes: R5 but not X4 viruses replicate in the absence of T-cell receptor restimulation. J. Virol. **73:**7515–7523.
48. **Williams, O., and H. J. Brady.** 2001. The role of molecules that mediate apoptosis in T-cell selection. Trends Immunol. **22:**107–111.
49. **Wykrzykowska, J. J., M. Rosenzweig, R. S. Veazey, M. A. Simon, K. Halvorsen, R. C. Desrosiers, R. P. Johnson, and A. A. Lackner.** 1998. Early regeneration of thymic progenitors in rhesus macaques infected with simian immunodeficiency virus. J. Exp. Med. **187:**1767–1778.
50. **Zack, J. A., S. J. Arrigo, S. R. Weitman, A. S. Go, A. Haislip, and I. S. Y. Chen.** 1990. HIV-1 entry into quiescent primary lymphocytes: molecular analysis reveals a labile, latent viral structure. Cell **61:**213–222.
51. **Zack, J. A., A. M. Haislip, P. Krogstad, and I. S. Y. Chen.** 1992. Incompletely reverse-transcribed human immunodeficiency virus type 1 genomes in quiescent cells can function as intermediates in the retroviral life cycle. J. Virol. **66:**1717–1725.